Anodic Performance and Intermediate Temperature Fuel Cell Testing of $La_{0.75}Sr_{0.25}Cr_{0.5}Mn_{0.5}O_{3-\delta}$ at Lanthanum Gallate Electrolytes

J. Peña-Martínez,[†,‡] D. Marrero-López,[†] J. C. Ruiz-Morales,[†,‡] C. Savaniu,[‡] P. Núñez,*[,†] and J. T. S. Irvine*[,‡]

Inorganic Chemistry Department, University of La Laguna, 38200 La Laguna, Tenerife, Canary Islands, Spain, and School of Chemistry, University of St. Andrews, Fife KY16 9ST, Scotland, U.K.

Received July 28, 2005. Revised Manuscript Received December 3, 2005

This study is focused on the electrochemical performance of perovskite-type materials based on doped $LaGaO_3$ (LGO). $La_{0.9}Sr_{0.1}Ga_{0.8}Mg_{0.2}O_{3-\delta}$ (LSGM) and $La_{0.9}Sr_{0.1}Ga_{0.8}Mg_{0.115}Co_{0.085}O_{3-\delta}$ (LSGMCo) were used as electrolytes and $La_{0.8}Sr_{0.2}MnO_{3-\delta}$ (LSM) and $La_{0.75}Sr_{0.25}Cr_{0.5}Mn_{0.5}O_{3-\delta}$ (LSCM) as cathode and anode material, respectively. Much better performance was obtained at an LSGM electrolyte than at LSGMCo, probably due to interfacial reactions between LSGMCo and LSM. An LSGM electrolyte was prepared by tape casting with a thickness of about 120 μm and good values of power output in a conventional electrolyte-supported cell were achieved, 425 and 570 mW/cm^2 using wet 5% H_2/Ar and pure hydrogen as fuel, respectively, and pure O_2 as oxidant at 1073 K.

1. Introduction

Fuel cells are highly promising energy conversion systems for the new energy economy and especially in the future hydrogen scenery. The key advantage of fuel cells is high efficiency from a range of system sizes. Systems are being commercially developed from sub-kW to 10 MW. Solid oxide fuel cells (SOFCs) are of particular interest due to their fuel flexibility. For many applications such as combined cycle with gas turbines and heat cogeneration, the high SOFC temperatures up to 1273 K offer significant advantages. These high temperatures present significant problems for materials selection and durability, especially for smaller scale applications; thus, there is also considerable impetus to develop lower temperature SOFC systems. A decrease in the operation temperature means a loss of power density mainly due to a considerable reduction of both ionic conductivity of the electrolyte and catalytic activity of the electrodes. To avoid ohmic loss, the thickness of the electrolyte might be reduced or alternative electrolyte materials used, providing that they offer good performance for operation at intermediate temperatures (773−1073 K). For example, it is necessary to reduce the thickness of yttrium-stabilized zirconia (YSZ) electrolyte to at least 15 μm to achieve comparable performances at 973 K.[1]

Similarly, new electrode materials with enhanced electrode performance at lower temperatures should be achieved.

Much attention has been given to the search for different electrolyte materials, e.g., with fluorite-type structure (AO_2), such as gadolinium-doped ceria (CGO), which has a higher ionic conductivity than YSZ at intermediate temperatures.[2] However, this material has been reported to have short-circuit problems in low oxygen partial pressures due to partial reduction of Ce^{4+} to Ce^{3+} and so increasing n-type conductivity.[3] The ionic domain dominates at 773 K and below and hence gadolinia ceria is well-suited to operation at these temperatures, especially if a suitable cathode material is found for this temperature range.[4]

The versatile perosvkite-type structure (ABO_3) based on the doped $LaGaO_3$ (LGO) is another interesting option as electrolyte. A good ionic conductor was found by doping with Sr^{2+} and Mg^{2+} in the A- and B-site positions of the perovskite, creating oxygen vacancies as a consequence of the doping.[5] The best ionic conductivity was found in $La_{0.8}Sr_{0.2}Ga_{0.83}Mg_{0.17}O_{2.815}$ composition,[6] although $La_{0.9}Sr_{0.1}Ga_{0.8}Mg_{0.2}O_{2.85}$ (LSGM) is usually the preferred one.[7−9] In any case, LSGM is a better ionic conductor than YSZ at intermediate temperatures. Nevertheless, there are disadvantages such as undesired segregation of impurities during the synthesis procedure, e.g., $LaSrGa_3O_7$ and $LaSrGaO_4$,[10] and there is a reported chemical incompatibility with Ni-based anodes.[11,12] To date, it is necessary to use a buffer layer of

* To whom correspondence should be addressed. E-mail: pnunez@ull.es (P.N.) or jtsi@st-and.ac.uk (J.T.S.I.).
† University of La Laguna.
‡ University of St. Andrews.

(1) Steele, B. C. H.; Heinzel, A. *Nature* **2001**, *414*, 345−352.
(2) Steele, B. C. H. In *High Conductivity Solid Ionic Conductors*; Takahashi, T., Ed.; World Scientific: Singapore, 1989.
(3) Inaba, H.; Tagawa, H. *Solid State Ionics* **1996**, *83*, 1−16.
(4) Shao, Z.; Haile, S. M. *Nature* **2004**, *431*, 170−173.
(5) Ishihara, T.; Matsuda, H.; Takita, Y. *J. Am. Chem. Soc.* **1994**, *116*, 3801−3803.
(6) Huang, K.; Tichy, S. R.; Goodenough, J. B. *J. Am. Chem. Soc.* **1959**, *81*, 2565−2575.
(7) Ishihara, T.; Matsuda, H.; Azni, M.; Takita, Y. *Solid State Ionics* **1996**, *86−88*, 197−201.
(8) Fukui, T.; Ohara, S.; Murata, K.; Yoshida, H.; Miura, K.; Inagaki, T. *J. Power Sources* **2002**, *106*, 142−145.
(9) Kim, J. H.; Yoo, H. I. *Solid State Ionics* **2001**, *140*, 105−113.
(10) Matraszek, A.; Singheiser, L.; Kobertz, D.; Hilpert, K.; Miller, M.; Schulz, O.; Martin, M. *Solid State Ionics* **2004**, *166*, 343−350.

10.1021/cm0516659 CCC: $33.50
Published on Web 01/14/2006

CGO or samarium-doped ceria (SDC) between LSGM and Ni-based anodes in order to avoid the formation of impurities such as $LaSrGa_3O_7$ and lanthanum−nickel oxide.[13−15]

A new electrolyte material has been prepared and characterized in the literature,[16] based on LSGM, but with the addition of Co^{2+} in the B site of the perovskite structure, i.e., $La_{0.9}Sr_{0.1}Ga_{0.8}Mg_{0.115}Co_{0.085}O_{3-\delta}$ (LSGMCo). Ishihara et al.[17] reported that the cobalt doping is effective for enhancing the oxide ion conductivity at low temperature compared to LSGM. Recent work[18] has demonstrated that $La_{0.75}Sr_{0.25}Cr_{0.5}Mn_{0.5}O_{3-\delta}$ (LSCM)[19−21] can be utilized as an appropriate anode with a LSGMCo electrolyte; however, the performance was limited by the performance of the gadolinium strontium cobaltite (GSC) cathode and the fairly thick electrolyte, 0.5 mm. The cobaltite cathode was chosen for the initial study due to its anticipated compability with LSCMCo and most importantly its high reported performance on gadolinia ceria.[22] Unfortunately, the GSC is expected to exhibit much higher thermal expansion ($15-18 \times 10^{-6}$ K^{-1}) than LSCM and LSGM or LSGMCo ($\sim(10 \pm 1) \times 10^{-6}$ K^{-1}) and the lattice volume which is about 6% smaller than LSCM and LSGM (or LSGMCo) which are within 1−2% of each other.[18]

In this work LSGM and LSGMCo were tested as electrolytes using $La_{0.8}Sr_{0.2}MnO_{3-\delta}$ (LSM) and $La_{0.75}Sr_{0.25}Cr_{0.5}Mn_{0.5}O_{3-\delta}$ (LSCM) as cathode and anode, respectively. LSM is well-known as a stable SOFC cathode, although it does not exhibit the same degree of mixed conductivity as its cobalt analogue; however, it is much better matched in terms of thermal expansion coefficient, $\sim 12 \times 10^{-6}$ K^{-1}.[23] Furthermore, the primitive perovskite unit cell volume of LSM is 58.8 $Å^3$, only 1% different from that of either LSCM or LSGM.[18]

2. Experimental Procedures

2.1. Electrolyte and Electrode Preparation. LSGM and LSGMCo electrolytes and LSCM anode material have been prepared by conventional solid-state reaction using powders of La_2O_3 (Alfa Aesar, 99.99%), Ga_2O_3 (Alfa Aesar, 99.999%), $(MgCO_3)_4 \cdot Mg(OH)_2 \cdot 5H_2O$ (Aldrich, 99%), $SrCO_3$ (Aldrich, 99.9%), $Co(Ac)_2 \cdot 4H_2O$ (Panreac, 98%), Mn_2O_3 (Aldrich 99%), and $Cr(NO_3) \cdot 9H_2O$ (ACROS, 99%); commercial powders of LSM (Praxair, 99.9%) were used as cathode. Before weighing, La_2O_3 was predried at 1273 K for more than 3 h in order to achieve decarbonation.

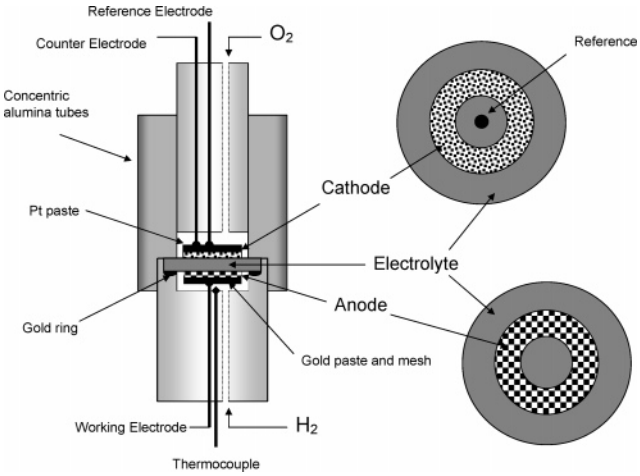

Figure 1. Three-electrode setup for polarizations measurements.

The stoichiometric quantities of reactants were ball-milled with acetone for the preparation of both electrolyte and anode materials. The resulting dried mixture was fired at 1173 K for 10 h and grounded again to obtain fine powders. LSCM powders were prepared via calcination at 1373 K (10 h) and LSGM and LSGMCo electrolytes were prepared as dense pellets (99% of theoretical density) by sintering at 1623−1673 K for 6 h in air after uniaxial pressing.

2.2. Tape Casting Preparation. The procedure for obtaining LSGM by tape casting samples comprised the preparation of a slurry containing powder, methylethyl ketone (MEK) as solvent; Triton QS-44 (phosphate ester, acid form) as dispersant to reduce the interfacial tension between the surface of the particle and the liquid; di-*n*-butyl phthalate (DBP) as plasticizer to increase the flexibility of the tapes; and BUTVAR B-98 as binder to provide their strength after the evaporation of the solvent. Intermediate ball-milling steps are used for the preparation of the tapes that are finally cut into disks and sintered at 1573 K with a slow heating rate. The thin electrolytes for fuel cell testing were prepared by laminating two layers of LSGM and firing both together at 1573 K to obtain a dense and homogeneous layer of 120 μm thickness after the firing.

2.3. Material Characterization. X-ray diffraction patterns (XRD) were collected with a Philips X'Pert Pro diffractometer, equipped with a primary monochromator and a Philips X'Celerator detector. The scans were performed in the high-resolution mode in the 2θ range from 20 to 70° (step 0.016° and 500 s/step), using Cu $K\alpha_1$ radiation. Scanning electron microscopy (SEM) and energy dispersive X-ray spectroscopy (EDS) were performed on JEOL JSM-5600 and Oxford INCA Energy 200 devices to characterize materials before and after tests. XRD studies were made to investigate the chemical compatibility of the electrolyte with the electrodes. Mixtures of LSGM with LSCM and LSM powders were prepared, in a 1:1 (w/w) ratio, ground in an agate mortar, and fired at several temperatures for 10 h. Additionally, the redox stability of LSGM was studied by XRD after exposing the sample to a wet H_2 flow at 1073 K for 48 h.

2.4. Electrochemistry Measurements. Polarization impedance and anodic overpotential fuel cell tests were carried out on a three-electrode arrangement (Figure 1) using 20 mm diameter LSGM pellets (2 mm thick) as electrolyte, LSM as cathode material, and LSCM as anode. The anode was prepared by coating a layer of

(11) Guillodo, M.; Vernoux, P.; Fouletier, J. *Solid State Ionics* **2000**, *127*, 99−107.
(12) Feng, M.; Goodenough, J. B.; Huang, K.; Milliken, C. *J. Power Sources* **1996**, *63*, 47−51.
(13) Huang, K.; Wan, J.; Goodenough, J. B. *J. Electrochem. Soc.* **2001**, *148*, A788−A794.
(14) Huang, K.; Goodenough, J. B. *J. Alloys Compd.* **2000**, *303−304*, 454−464.
(15) Stöver, D.; Buchkremer, H. P.; Uhlenbruck, S. *Ceram. Int.* **2004**, *30*, 1107−1113.
(16) Ishihara, T.; Shibayama, T.; Ishikawa, S.; Hosoi, K.; Nishiguchi, H.; Takita, Y. *J. Eur. Ceram. Soc.* **2004**, *24*, 1329−1335.
(17) Ishihara, T.; Furutani, H.; Honda, M.; Yamada, T.; Shibayama, T.; Akbay, T.; Sakai, N.; Yokokawa, H.; Takita, Y. *Chem. Mater.* **1999**, *11*, 2081−2088.
(18) Tao, S. W.; Irvine, J. T. S.; Kilner, J. A. *Adv. Mater.* **2005**, *17*, 1734−1737.
(19) Tao, S. W.; Irvine, J. T. S. *Nat. Mater.* **2003**, *2*, 320−323.
(20) Tao, S. W.; Irvine, J. T. S. *J. Electrochem. Soc.* **2004**, *151*, A252−A259.
(21) Zha, S.; Tsang, P.; Cheng, Z.; Liu, M. *J. Solid State Chem.* **2005**, *178*, 1847−1853.
(22) Ralph, M.; Rossignol, C.; Kumar, R. *J. Electrochem. Soc.* **2003**, *150*, A1518.
(23) Srilomsak, S.; Schilling, D. P.; Anderson, H. U. *Proceedings of the 1st International Symposium on Solid Oxide Fuel Cells*; The Electrochemical Society: Pennington, NJ, 1989; pp 129−140.

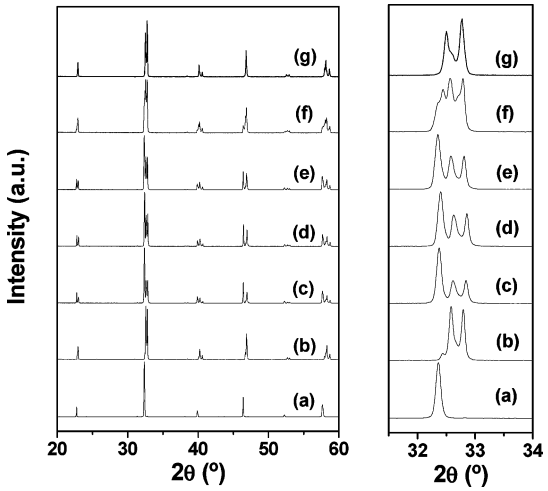

Figure 2. XRD patterns of LSGM (a), LSCM (b), and LSGM + LSCM at the following temperatures: room temperature (c), 1173 K (d), 1373 K (e), 1623 K (f), and 1773 K (g).

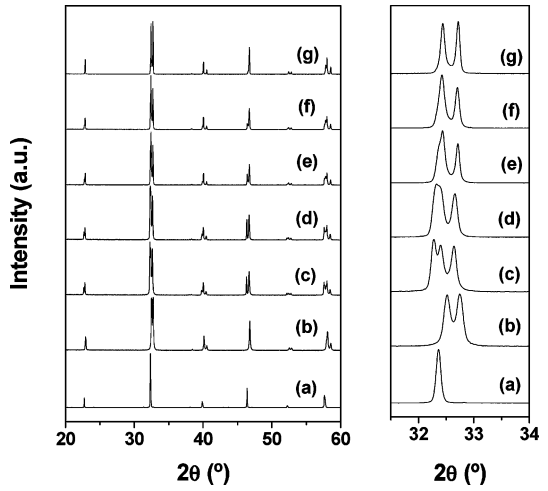

Figure 3. XRD patterns of LSGM (a), LSM (b), and LSGM + LSM at the following temperatures: room temperature (c), 1173 K (d), 1373 K (e), 1473 K (f), and 1673 K (g).

LSCM slurry, using Decoflux as binder, onto the electrolyte and then firing at 1573 K for 2 h in air. LSM was painted onto the other side of LSGM as counter-electrode and fired at 1473 K for 2 h. A gold current collector layer was used to avoid any additional catalytic effect and it was applied onto the working electrode by brushing Au paste with Au mesh on top. Platinum paste was used as a reference electrode and current collector on the cathode side. Finally, the specimen was fired at 1173 K for 2 h.

The three-electrode setup consists of 1 cm^2 aligned working and counter ring electrodes with a point reference placed at the center of the counter-electrode ring (Figure 1). Gold rings were used for sealing at 1198−1223 K. ac impedance of the electrochemical cell was acquired using a Zahner IM600 unit at open circuit voltage (OCV) in the frequency range 0.1 Hz to 1 MHz. An ac perturbation of 20 mV was used, obtaining reproducible spectra. The impedance of the single cell was measured under asymmetric atmospheres at open circuit conditions.

Fuel-cell performance was investigated using a 120 μm thick LSGM electrolyte prepared by tape casting. A two-electrode setup was used to obtain the $I-V$ plots using wet 5% H_2 and 100% H_2 gases as fuels and O_2 as oxidant. The anode and cathode were LSCM and LSM, respectively, and both were deposited in the same way as in the three-electrode arrangement. The fuel cell performance

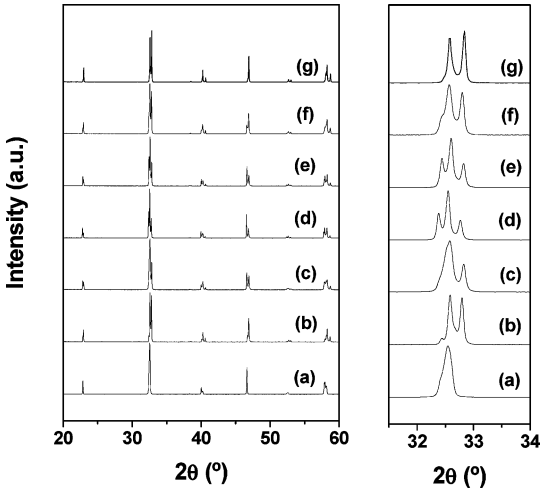

Figure 4. XRD patterns of LSGMCo (a), LSCM (b), and LSGMCo + LSCM at the following temperatures: room temperature (c), 1173 K (d), 1373 K (e), 1623 K (f), and 1773 K (g).

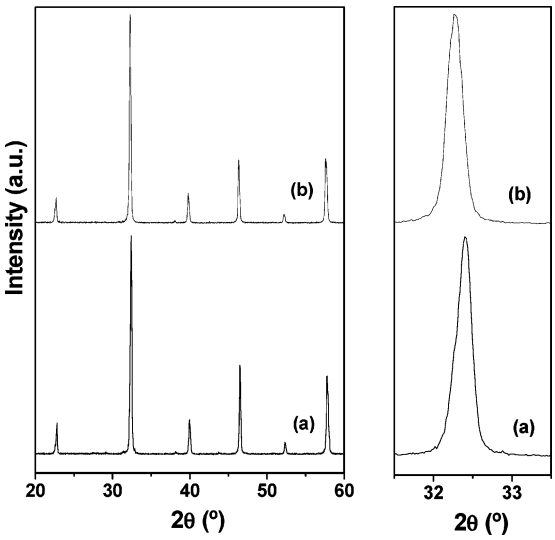

Figure 5. XRD patterns of LSGM in air at room temperature (a) and after exposure in a wet H_2 atmosphere (b) at 1073 K for 48 h.

was recorded by cyclic voltammetry at a scan rate of 4 mV s^{-1}. Electrochemical tests were performed after reducing the anode materials in 5% H_2 at 1073 K for several hours.

3. Results and Discussions

3.1. Chemical Compatibility. XRD patterns of the reacted intimate mixtures of LSGM/LSCM, LSGMCo/LSCM, and LSGM/LSM pressed powders are shown in Figures 2, 3, and 4. Certain reactivity could be observed between LSM and LSGM above 1373 K, between LSGM and LSCM at 1623 K, and between LSGMCo and LSCM above 1173 K. No reaction was observed for the LSGM/LSCM system at 1173 K. In this sense, Du and Sammes[24] reported that no interactions were detected from XRD data in their experiments of fabrication of bilayer samples of LSGM and LSCM at 1773 K for 2 h; however, they found severe reactions in samples after 6 h and over at 1773 K, forming low

(24) Du, Y.; Sammes, N. M. *Proceedings of the 9th International Symposium on Solid Oxide Fuel Cells (SOFC-IX)*; The Electrochemical Society, PV 2005-07- ISBN 1-56677-465-9, Solid Oxide Fuel Cells (SOFC-IX), 2005; p 1127.

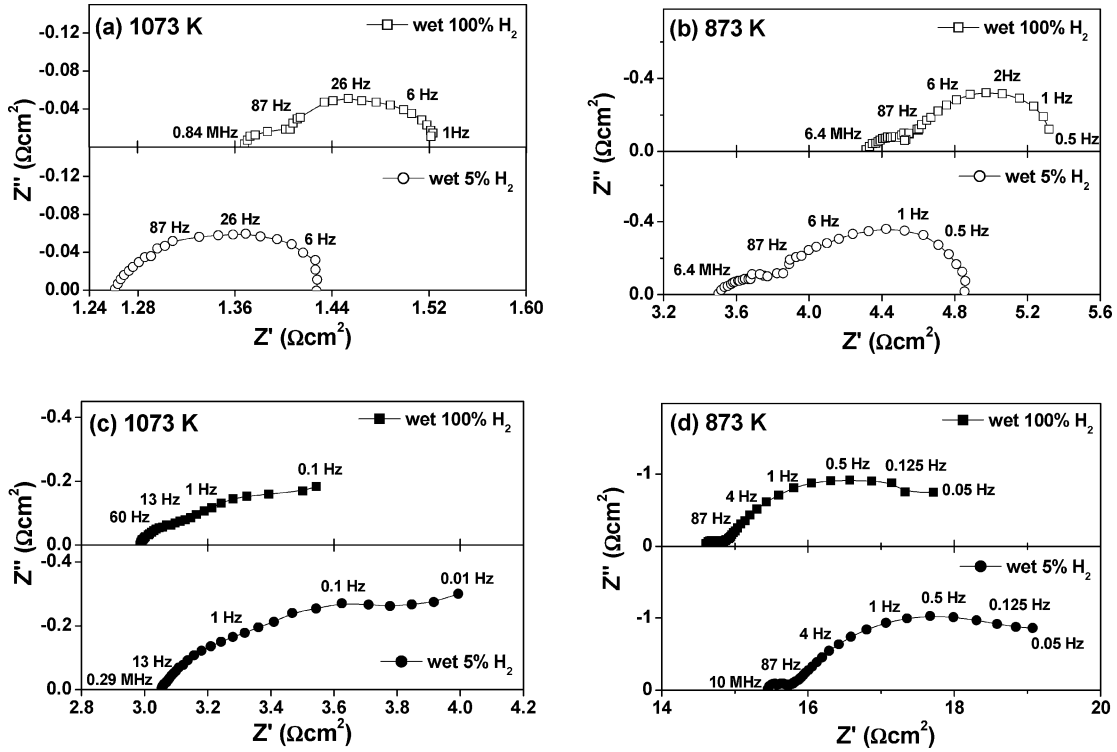

Figure 6. Polarization resistances for LSGM (open symbol) and LSGMCo (closed symbol) in different gas compositions, wet 100% H_2 (square), and wet 5%H_2/Ar (circle), at 1073 K (a, c) and 873 K (b, d).

conductive phases. They used energy-dispersive spectrometry (EDS) analysis to find reaction−diffusion zones in the range 50−150 μm. Nevertheless, they indicate from their overall results that LSCM is a thermomechanically and chemically compatible anode material with LSGM electrolyte at the fuel cell operating temperatures and fuel cell fabrication conditions (at 1773 K for 2 h). In this work LSCM material has been applied to the electrolyte at 1623 K for 2 h, and LSGM and LSCM did not show apparently remarkable signs of reaction in fired compacted powder. However, the XRD pattern of the mixture LSGM/LSCM at 1623 K for 10 h, Figure 2f, showed a reaction which becomes stronger at 1773 K, Figure 2g. The interaction between LSGM/LSCM has not been studied further and more studies are necessary. In the LSM/LSGM case, previous studies on the interface between LSM and LSGM have shown that a reaction layer is formed between them and the thickness of the layer increased with the sintering temperature.[25] Huang et al.[13] reported that the high diffusion of La in LSGM electrolytes can modify the LSGM composition, leading to the formation of resistive phases such as $LaSrGa_3O_7$ or $LaSrGaO_4$, at the electrolyte/electrode interfaces depending on whether La diffuses out of or into LSGM. The LSM electrode fired at 1473 K onto LSGM did not show obvious signs of reaction; however, based upon the powder mixture studies, it is anticipated that some interdiffusion will have occurred at the interface.

In addition, there are no noticeable changes or extra peaks (Figure 5) on exposure of LSGM to wet H_2 at 1073 K for 48 h. This is in accord with the good stability in reducing conditions reported by Huang and Goodenough.[14]

(25) Yeon, J. Y.; Choi, G. M. *J. Eur. Ceram. Soc.* **2004**, *24*, 1359−1363.

3.2. Fuel Cell Tests. *3.2.1. Series and Polarization Resistances.* The polarization resistances for LSCM at a LSGM electrolyte were 0.15 and 0.16 Ωcm^2 at 1073 K in 3% H_2O/97% H_2 and 3% H_2O/4.8% H_2/92.2% Ar, respectively; see Figure 6a. These values are lower than those obtained by Tao et al.[19] at 1223 K on YSZ, indicating an enhancement at the perovskite/perovskite interface as previously reported by Tao et al.[18] at LSGMCo; however, the polarization resistances in the experiments reported here are considerably lower, perhaps indicating that improved processing was yielding better microstructures or that the presence of Co was downgrading performance. Even at 873 K the values of polarization resistance were not that high, being 1.0 and 1.4 Ωcm^2 in 3% H_2O/97% H_2 and 3% H_2O/4.8% H_2/92.2% Ar, respectively, Figure 6b. The results using LSGMCo were poor by comparison to LSGM and were slightly worse than those previously reported for LSGMCo using a thick pellet electrolyte.[18] Compared to the LSGM data and the previous LSGMCo report in this instance, it was more difficult to obtain the intercept at low frequencies from the impedance plots, Figures 6c and 6d. This indicates a large diffusion reaction, which could be in accord with the low conductive phases and a reaction/diffusion zone discovered by Du and Sammes at the LSGM/LSCM interface.[24] Tao et al.[18] reported that a slight cross-diffusion at the LSGMCo/LSCM interface may occur during long-term operation. The likely reaction/diffusion area at the LSGMCo/LSCM interface seems to be the key to finding an explanation for the impedance spectra behavior. More measurements are now under investigation in order to clarify this reaction.

Furthermore, the series resistance increases in the reducing conditions for LSGM-electrolyte samples, Figure 6a,b. The

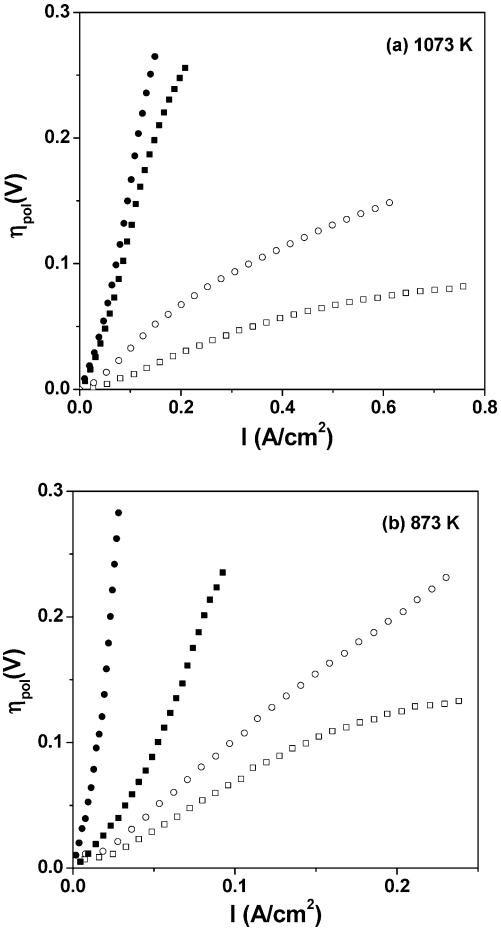

Figure 7. Anodic overpotential plots for LSGM (open symbol) and LSGMCo (closed symbol) at 1073 K (a) and 873 K (b) in different gas compositions: wet 100% H_2 (square) and wet 5%H_2/Ar (circle).

increase in the series resistance in reducing conditions could be explained by the loss of conductivity for LSCM when decreasing the pO_2 (p-conductivity);[19] i.e., the total conductivity is lower and this may well be amplified by the interlayer described below from SEM investigation of this system. In contrast, the series resistance increases under reducing conditions for the LSGMCo-electrolyte samples, Figure 6c,d. Ishihara et al.[26,27] suggest that some p-conductivity can be assigned to the formation of Co^{3+} and the oxidation state of Co changes from +3 to +2 when decreasing oxygen partial pressure, leading to a loss of conductivity. In addition, the formation of an interdiffusion layer between the anode and the electrolyte, in reducing conditions, could affect the total conductivity of the samples.

3.2.2. Anodic Overpotential. The anodic overpotentials for LSCM at the LSGM electrolyte, Figure 7a, were 28 and 67 mV, at 0.2 A/cm^2, at 1073 K, in wet H_2 and wet 5%H_2/Ar, respectively. At 873 K, these values are 125 and 200 mV, at the same current density in wet H_2 and wet 5%H_2/Ar, respectively. In contrast, the overpotentials for LSGMCo-electrolyte samples were too high, see Figure 7. Thus, the performance was lower compared to LSGM-electrolyte samples. One possible explanation for this poor performance

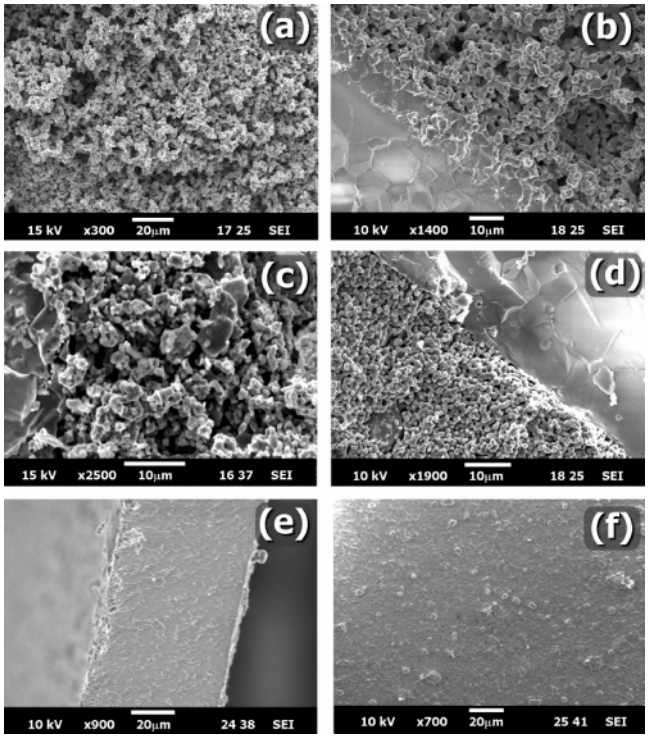

Figure 8. SEM images showing the LSCM anode of a fuel cell after testing, using LSGM as electrolyte, (a) top section, (b) cross section, and LSGMCo as electrolyte, (c) cross section. LSM cathode of a fuel cell using LSGM as electrolyte, (d) cross section. Cross section (e) and surface (f) of a sintered layer of LSGM electrolyte prepared by tape casting.

is likely to be due to the poor contact between anode and electrolyte, Figure 8c.

3.2.3. Power Density. High fuel cell performances are expected from these obtained overpotentials using LSGM as electrolyte and LSCM as anode. In fact, fuel cell tests using thin electrolyte, Figure 9a,b, show high performances at 1073 K in either pure hydrogen, 570 mW/cm^2, and 425 mW/cm^2 in 5% H_2/Ar. At 873 K the electrical performance drops to around 120−160 mW/cm^2. Again the performance in 5%H_2/Ar is about 75% of the value obtained with pure hydrogen. Fukui et al.[8] reported a power density over 0.7 W/cm^2 at 1073 K and 0.4 W/cm^2 at 973 K in a cell with LSGM as electrolyte of ∼130 μm of thickness prepared by tape casting, $La_{0.6}Sr_{0.4}CoO_{3-\delta}$ (LSC) as cathode and NiO−$(CeO_2)_{0.8}(SmO_{0.15})_{0.2}$ (NiO−SDC) as anode material using 97%H_2 + 3%H_2O as fuel and air as oxidant. Our value of power density at 1073 K is in the same range of Fukui values, although it is important to notice the differences on the used electrodes and the oxidant gas.

Our data are also in accord with the preliminary tests of Goodenough and co-workers,[28,29] who obtained a 430 mW/cm^2 power output at 1073 K with CH_4 as fuel using $SrCo_{0.8}Fe_{0.2}O_{3-\delta}$ as cathode, $La_{0.8}Sr_{0.2}Ga_{0.83}Mg_{0.17}O_{2.815}$ as electrolyte, and LSCM as anode material.

SEM pictures were taken after performing the fuel cell tests to investigate the microstructure of the different

(26) Ishihara, T.; Akbay, T.; Furutani, H.; Y. Takita, Y. *Solid State Ionics* **1998**, *113*−*115*, 585−591.
(27) Ishihara, T.; Ishikawa, S.; Ando, M.; Nishiguchi H.; Takita, Y. *Solid State Ionics* **2004**, *173*, 9−15.
(28) Wan, J.-H.; Yan, J.-Q.; Goodenough, J. B. *J. Electrochem. Soc.* **2005**, *152* (8), A1511−1515
(29) Wan, J.-H.; Zhu, J. H.; Goodenough, J. B. *Proceedings of the 9th International Symposium on Solid Oxide Fuel Cells (SOFC-IX)*; The Electrochemical Society, PV 2005-07- ISBN 1-56677-465-9, Solid Oxide Fuel Cells (SOFC-IX), 2005; p 429.

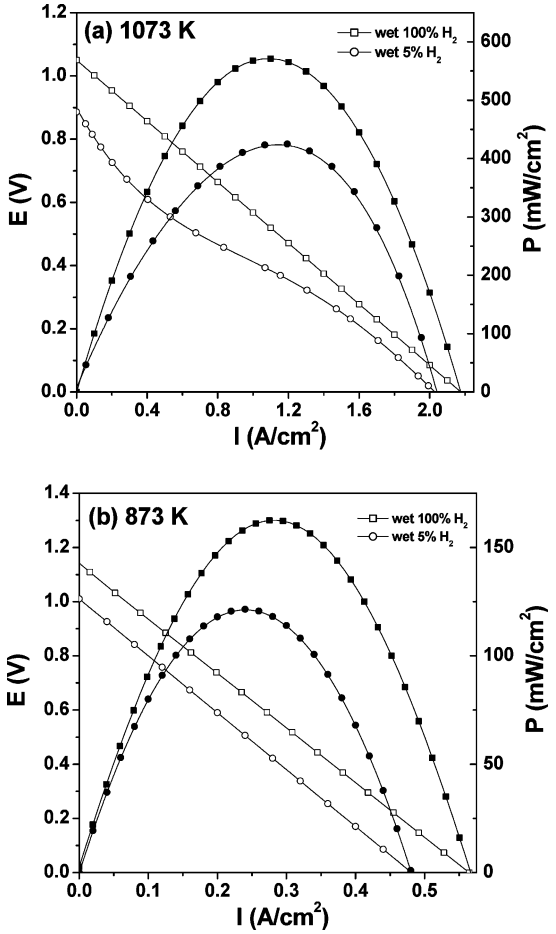

Figure 9. Performance (closed symbol) and $I-V$ (open symbol) curves, in different gas compositions with 3% of water, 100% H_2 (continuous line) (square), and 5% H_2 (dashed line) (circles), at 1073 K (a) and 873 K (b).

components and possible degradation or diffusion of the anode/cathode and electrolyte. The anode shows a homogeneous distribution of particles and pores with grain size ranging from 1 to 2 μm, see Figure 8a,b. Thus, the ohmic overpotential due to the contact resistance can be neglected because the adherence seems to be good, as seen in Figure 8b. A loss of performance could be expected as it looks like there is a possible reaction between the anode and electrolyte, leading to the formation of a 10 μm interdiffusion layer (Figure 8b). Microstructure and adherence of the LSM cathode also seem good (Figure 8d); however, the LSM/LSGM XRD study indicated possible interfacial reaction which could affect the electrical performance of the cell.

Figure 8e illustrates the cross section over 60 μm and relative density around 99% of a sintered layer of LSGM electrolyte prepared by tape casting. Figure 8f shows the surface of this layer of LSGM with an average grain size of 2.5 μm.

SEM pictures taken on LSGMCo cells, after tests, show that the contact between the anode and electrolyte was poor (Figure 8c) and seem to show more than one particle morphology. These factors could explain the high polarization resistances obtained using this electrolyte and processing route. Tao et al. recently reported[18] that the diffusion of the transition elements such as Cr, Mn, and Co into the LSGMCo electrolyte is insignificant at LSGMCo/LSCM interfaces. They studied these interfaces with an inductively coupled plasma mass spectrometer (ICP-MS). On the other hand, a strong reactivity between the LSGMCo and LSCM mixture can be observed in their XRD pattern at 1173 K and above in Figure 4.

4. Conclusions

Current−potential, current power-density, anodic losses, and overpotential of the LSM/LSGM/LSCM and LSM/LSGMCo/LSCM cells were investigated in this study at 1073 and 873 K using wet pure hydrogen and 5%H_2/Ar as fuels and O_2 as oxidant. The performance of LSM/LSGMCo/LSCM at 1073 K was inferior to the performance obtained on LSM/LSGM/LSCM at 873 K in both H_2-containing atmospheres. The power-density value for the LSM/LSGM/LSCM system with 5%H_2/Ar was 75% of the value obtained for the pure H_2 case and the maximum power density was 570 mW/cm^2 at 1073 K with an electrolyte thickness of about 120 μm.

Acknowledgment. The authors acknowledge financial support from EU Marie Curie (Contract No. HPMT-CT-2002-02001), European Science Foundation Program OSSEP, Spanish Research Program (MAT2001-3334 and MAT2004-3856 projects), Canary Islands Government (PI2004/093 and PhD grants), and the EPSRC for a Platform grant.

CM0516659